Band Structure Engineering of Semiconductor Lasers for Optical Communications

E. YABLONOVITCH AND E. O. KANE

Abstract—**Recent advances in epitaxial growth have led to the prospect of artificial modification of the electronic structure or band structure of semiconductor materials. The combination of strain and quantum confinement in the valence band can lead to substantially more favorable energy dispersion relations for laser action than those existing in the natural semiconductor crystal. Numerical results are presented for a series of alloy compositions with a bandgap near the 1.55 μm optimum wavelength for optical communications. The laser threshold current and the intervalence band absorption can be significantly diminished in properly engineered band structures.**

INTRODUCTION

IT HAS BECOME apparent recently [1], [2] that the lowering of valence band effective mass can have considerable benefits for semiconductor lasers. The technology of band structure engineering, which includes superlattices, quantum confinement, and intentional incorporation of strain [3], has now become sufficiently advanced that it can be employed in a routine manner. We must regard the natural electronic band structure of the III-V semiconductor crystals as merely a starting point for application in devices. We can change the band structure in an artificial fashion to suit our needs. In this paper we extend previous work [1], [2] by presenting a series of band structure calculations on alloy compositions and strain layers which are likely to be important for semiconductor lasers employed in optical communications.

In semiconductor lasers the prime culprit is the very heavy valence band mass. Unfortunately, in the III-V semiconductors, there is a serious asymmetry between the very light conduction band mass and the heavy valence band mass. Ideally both masses should be as light as possible. The density of states would be very small and the carrier density required for degeneracy would be minimized. Then the Bernard–Duraffourg [4] condition could be satisfied at a low carrier density with accompanying benefits in terms of threshold current, nonradiative recombination, etc.

In real materials, the usual semiconductor laser picture [5] of a degenerate distribution of electrons and holes does not actually apply. The upper laser levels in the conduction band are indeed filled with degenerate electrons but the lower laser levels in the valence band are not empty. Due to the heavy valence band mass, the hole quasi-Fermi level is above the top of the valence band and the hole distribution is classical. This situation is illustrated in Fig. 1(a). Therefore, the hole occupation probability at the top of the valence band is small, i.e., the lower laser levels are almost completely filled with electrons.

Present day semiconductor lasers find themselves in the awkward position of lasing down from filled states to almost filled states. The more ideal situation of equal conduction and valence band mass is illustrated in Fig. 1(b). We seek to arrive at that situation by means of band structure engineering.

The top of the valence band at the Γ point of the Brillouin zone has the symmetry of an atomic $^2P_{3/2}$ wave function. The heavy valence band is equivalent to an $m = \pm 3/2$ state and the degenerate light valence band is equivalent to an $m = \pm 1/2$ state, accounting for the fourfold degeneracy at the Γ point. Degenerate levels are particularly susceptible to small perturbations. In this case, strain in the z-direction or quantum confinement in the z-direction can have the effect of splitting the degeneracy at the Γ point. Given the appropriate sign of strain, the light valence band can be shifted to lie above the heavy band, reducing the effective mass for holes.

The threshold condition for gain is the well known Bernard–Duraffourg [4] condition:

$$(F_c - F_v) > \hbar\omega \geq E_g \tag{1}$$

which requires that the separation of quasi-Fermi levels $(F_c - F_v)$ should be greater than the bandgap. In both Fig. 1(a) and (b), this condition is minimally satisfied. In practice, the quasi-Fermi level separation should exceed the minimal value by 1 or 2 kT in order to overcome cavity losses, etc., but this would not change any of our conclusions. The two-dimensional density of states per unit carrier energy per unit area is $m/\pi\hbar^2$ and is independent of carrier energy. Then the carrier injection level n per unit area required to produce the quasi-Fermi level separation in Fig. 1(b) is:

$$n = \int_0^\infty \frac{1}{e^{E/kT} + 1} \frac{m_c}{\pi\hbar^2} dE$$

$$n = \frac{kT\, m_c}{\pi\hbar^2} \ln 2. \tag{2}$$

The situation in Fig. 1(a) is more complex. The electrons are degenerate and their density is given by $n = m_c\Delta/\pi\hbar^2$,

Manuscript received July 27, 1987; revised October 26, 1987.

The authors are with Bell Communications Research, Navesink Research Center, Red Bank, NJ 07701-7020.

IEEE Log Number 8719189.

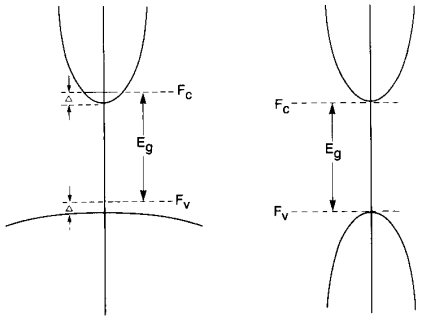

Fig. 1. On the left is the actual band structure of a typical III-V semiconductor. On the right is an idealized band structure in which the conditions for lasing can be more easily met. Due to the effective mass asymmetry on the left side, the quasi-Fermi levels are offset from the symmetrical position by an energy Δ. This requires an excess population of carriers as is evident by comparing the electron Fermi level on the left and on the right. When both hole and electron masses are light as on the right, the Bernard-Duraffourg condition is fulfilled at lower carrier injection.

where Δ is the degeneracy energy. The holes are nondegenerate and their density p can be approximated by:

$$p = \frac{kT\, m_c}{\pi\hbar^2} \exp\left\{-\frac{\Delta}{kT}\right\}. \tag{3}$$

Equating n and p results in an equation for Δ which can be solved iteratively on a hand calculator:

$$\left(\frac{\Delta}{kT}\right)\left(\frac{m_c}{m_h}\right) = \exp\left\{-\frac{\Delta}{kT}\right\}. \tag{4}$$

A reasonable value for (m_c/m_h) is $1/6$, which results in a value for $\Delta = 1.43$ kT. Therefore the ratio of injection level in the case in Fig. 1(a) divided by the case in Fig. 1(b) is $1.43/\ln 2$ which is a factor greater than two. The point is that the carrier injection level required for lasing is diminished in band structure engineered materials with equal hole and electron masses.

The greater ease of satisfying the Bernard–Duraffourg condition is not the only benefit from reducing the valence band mass. The changed band structure has other benefits as well. Of great concern in determining the laser threshold conditions is nonradiative recombination, especially in the form of Auger recombination in which two holes and an electron collide and recombine, leaving only one hole and some heat behind. This recombination process tends to proceed at a rate proportional the cube of carrier density. Obviously even a factor two reduction in injection level can produce almost an order of magnitude reduction in Auger recombination. But this actually understates the benefit. Not only is the carrier density reduced, but we will show that the Auger recombination coefficient itself will be reduced as well.

Another problem in semiconductor lasers involves not the threshold condition but rather the free carrier absorption which is present above the lasing threshold. Once again it is the free carrier absorption of the heavy holes in the form of intervalence band absorption which is the main culprit. We will show that the changes in band structure we are contemplating will act to reduce specifically that population of heavy holes which satisfies the momentum matching conditions for intervalence band absorption.

The one parasitic phenomenon in semiconductor lasers which will hardly be affected by band structure engineering is spontaneous emission. This is simply the ordinary radiative recombination of electrons with holes which contributes seriously to the current density required at threshold. According to the link between stimulated and spontaneous emission which was first demonstrated by Einstein through his A and B coefficients, if we are going to have lasing action it must be accompanied by spontaneous emission. Nevertheless there has been a proposal recently [5] to restrict the spontaneous emission, which usually propagates into all 4π, so that it accesses only the lasing mode and is inhibited in all other directions. Thereby, the radiative recombination at threshold could be reduced to a negligible level. Inhibited spontaneous emission is notoriously difficult to achieve experimentally. We will not address that problem by band structure engineering.

In order to develop a better understanding of intervalence band absorption and how we might influence it, it would be fruitful to examine Fig. 2. Shown are the top of the valence band region including the light and heavy holes and the spin orbit split off band. The energy difference Δ_o between the spin orbit split off band and the top of the valence band is ~ 0.35 eV for the important practical case of $In_{0.53}Ga_{0.47}As$. The leading intervalence band absorption process, shown in Fig. 2, competes seriously with stimulated emission once lasing has commenced above threshold. The need to simultaneously absorb a photon energy equal to the bandgap energy of 0.8 eV with hardly any accompanying momentum requires the transition to take place quite far from zone center. In particular, intervalence band absorption depends on the population of off zone center heavy holes which we can hope to influence through band structure engineering. This will be demonstrated later in the paper with specific energy band calculations.

Likewise, Auger recombination is also strongly dependent on the population of off zone center heavy holes as can be seen from Fig. 3. The leading Auger process CHSH, takes advantage of the spin orbit split off band to take up as much energy as possible with the least amount of momentum. CHSH stands for two holes and one electron recombining to produce an energetic hole on the spin orbit split off band. Conservation of energy and momentum implies that the two arrows in Fig. 3 must be antiparallel and of equal length. From the geometrical relationship shown in Fig. 3 it is clear that the process depends once again on the population of off-zone-center heavy holes which we can hope to influence by appropriately shaping the topmost valence band.

The conclusion is that three of the most troublesome aspects of semiconductor lasers; a) the asymmetry of conduction and valence band mass, b) intervalence band op-

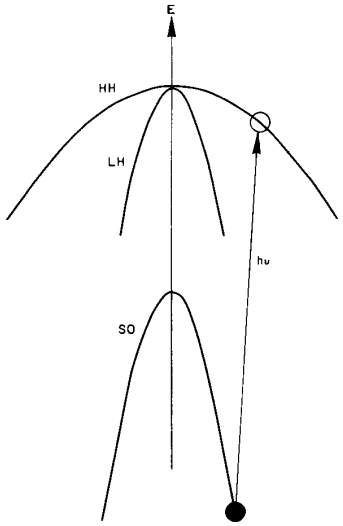

Fig. 2. Intervalence band absorption. The conservation of energy and momentum requires almost vertical transitions in the parasitic intervalence band absorption process which competes with laser gain. The dominant process, which is illustrated here, involves a transition from an electron in the spin-orbit split off band into a hole in the heavy valence band. The essential point is that the absorption is proportional to the population of off zone center heavy holes. Our goal is to diminish that population by changing the shape of the heavy valence band.

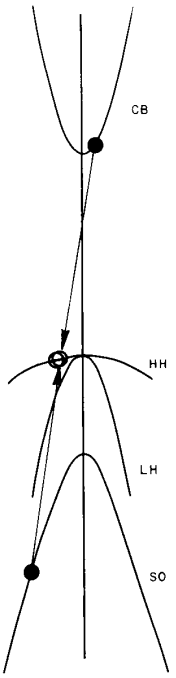

Fig. 3. Auger recombination which is a major current sink, also requires energy and momentum conservation. This is a three body process, the dominant version being the CHSH process, in which two heavy holes recombine with one free electron leaving a hole behind in the spin-orbit split off band. This process is proportional to the square of the off zone center heavy hole population and can be strongly influenced by the shape of the heavy hole band.

tical absorption and c) Auger recombination, can all be addressed by changing the valence band structure to reduce mass and reduce the population of heavy holes. With that motivation we can now consider practical cases with specific materials in mind.

Band Structure Engineering

We will be guided by a desire to engineer a bandgap to match the dominant wavelength in optical communications which occurs at 1.55 μm, corresponding to a photon energy of 0.8 eV. Among the III-V semiconductors, this energy condition already restricts us to those compounds with a lattice constant larger than the 5.8688-Å lattice constant of InP. All those materials with a smaller lattice constant have larger bandgaps. Among the larger lattice constants are the alloys based on GaSb which include mixtures of As and Sb. These are relatively less studied, and would present problems since we will require negative strain such that the active alloy will have to have a unstrained lattice constant larger than that of the substrate on which it is grown. The most practical course therefore is to restrict our attention to the well studied alloys of the type: $In_xGa_{1-x}As$ with x in the composition range $0.53 \leq x \leq 1.0$. These relatively well studied alloys have a good materials growth technology, and are strained in the right direction to raise the light valence band above the heavy band when grown on InP. Furthermore we can anticipate that the quantum size effect which will increase the bandgap can be almost exactly balanced against the lower gap of the In-rich alloy compositions to produce a bandgap around 0.8 eV.

In order to conduct band structure engineering it is necessary to input a host of materials constants for GaAs, InAs and the intermediate alloys. We found that the excellent compilation edited by Madelung [7] was invaluable in providing the fullest possible set of materials parameters. These are presented in Table I. The Kohn-Luttinger parameters γ_n express what is known about the valence band masses in the natural III-V crystals. An unknown parameter in the table was γ_3 of $In_{0.53}Ga_{0.47}As$. It was simply set equal to γ_2 which is equivalent to neglecting the anisotropy of the valence band mass. The a, b, and C_{12}/C_{11} constants of $In_{0.53}Ga_{0.47}As$ were set by interpolation from the two binary compounds. The deformation potential "a" describes the change in bandgap due to hydrostatic strain deformation. We will be exclusively considering growth in the ⟨100⟩ direction. In epitaxial growth along a cubic axis the two horizontal axes are strained one way while the third vertical axis responds oppositely through Poisson's ratio. The change in bandgap is given by:

$$a \times [2\epsilon_{xx} - 2(C_{12}/C_{11})\epsilon_{xx}] \tag{5}$$

where the second term represents the induced strain along the z-direction. Similarly, the splitting between the light and heavy hole bands due to uniaxial strain may be represented by:

$$2b \times [\epsilon_{xx} + 2(C_{12}/C_{11})\epsilon_{xx}] \tag{6}$$

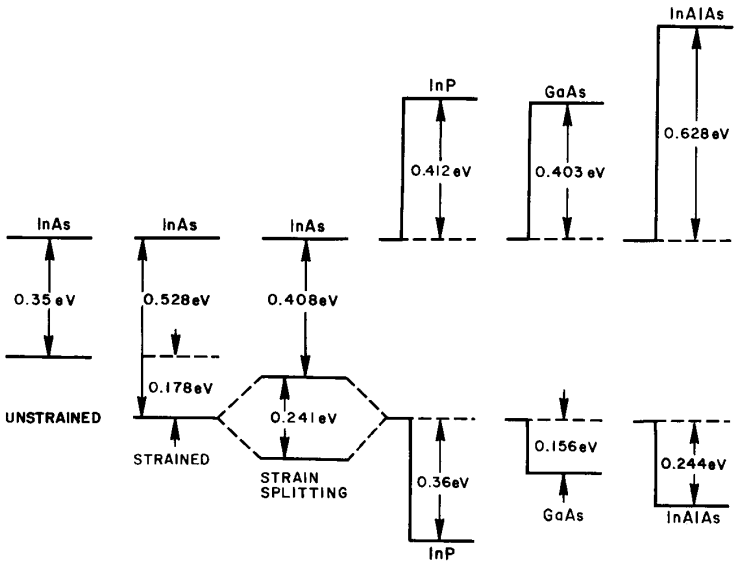

Fig. 4. The bandgaps and the band offsets assumed in these calculations. On the left is unstrained InAs. First the strain induced bandgap increase is shown, then the strain induced splitting of the degenerate valence band. (We do not mean to imply that the strain affects only the valence band.) The band offsets with respect to InP, GaAs, and $In_{0.52}Al_{0.48}As$, all lattice matched to InP are shown next. The bandgap of GaAs is adjusted for the strain but the valence band splitting is not displayed in this figure.

TABLE I
THE SPECIFIC VALUES OF MATERIAL PARAMETERS USED IN OUR CALCULATIONS
The strain ϵ_{xx} is specified with respect to growth on an InP substrate. The conduction band mass m_c is in units of the free electron mass. The γ_n are the Kohn–Luttinger parameters, a and b are the bandgap and valence band splitting deformation potentials respectively, and the C's are stiffness constants.

	GaAs	InAs	$In_{0.53}Ga_{0.47}As$
γ_1	6.95	19.67	10.8
γ_2	2.25	8.37	4.4
γ_3	2.86	9.29	4.4
m_c	0.069	0.023	0.041
a in eV	-8.23	-6	-7
b in eV	-2.0	-1.8	-1.9
C_{12}/C_{11}	0.45	0.54	0.5
E_g(300°K) in eV	1.42	0.35	0.75
Lattice Constant (Å)	5.6535	6.0585	5.8688
ϵ_{xx}	0.0367	-0.0323	0

where the second term representing induced strain along the z-direction now adds coherently to the uniaxial deformation. The splitting deformation potential is "b."

The effect on InAs zone center energy levels of strained growth on an InP substrate are shown on the left side of Fig. 4. First the hydrostatic strain bandgap shift is introduced and then the strain splitting of the valence band. For negative strain the heavy hole band will be split above the light hole band. Nevertheless the expression "heavy" is only meant to describe the angular momentum state $m = \pm 3/2$; the effective mass due to the uniaxial strain will actually be light in the plane and heavy in the z-direction.

We have conducted band structure calculations of the strained quantum wells. It is well known that the most serious problem in this field is the unavailability of accurate band edge discontinuities. We have made a critical reading of the literature and attempted to select reasonable numbers, which are presented on the right side of Fig. 4 for strained InAs with respect to the following three barrier layers: InP, strained GaAs, and $In_{0.52}Al_{0.48}As$. A good starting point is to observe that the valence band offsets (VBO) for InAs/GaAs is rather [8], [9] small, ~ 0.16 eV. This means that the VBO for the entire $In_{1-x}Ga_xAs$ alloy series can probably be approximated by linear interpolation and is small in any case. This information is very valuable when used in conjunction with the rather accurate VBO's that have been measured with respect to the midrange member of this alloy series, namely $In_{0.53}Ga_{0.47}As$. The VBO's for $In_{0.53}Ga_{0.47}As/InP$ and $In_{0.53}Ga_{0.47}As/In_{0.52}Al_{0.48}As$ are among the most repeatable and reproducibly measured [10], [11] numbers in the band offset field. If we make the assumption of transitivity [8] then the VBO of all the different members of these alloy groups is determined. The values of band offsets given on the right side of Fig. 4 are not representative of any one experimental determination nor are they necessarily the best available values, they are simply the values that were used in the calculations presented here. Fortunately, our calculations will show that the band structure

is not strongly dependent on the VBO as long as it exceeds ~0.2 eV. It should be noted that the valence band splitting for strained GaAs is not displayed in Fig. 4.

Our method of calculation is an adaptation of the approach of Nedorezov [12] in which the finite well depth for the valence band is explicitly incorporated. The wave function in the well and barrier regions is solved in the envelope approximation. Only the topmost fourfold degenerate valence band states (that is the heavy and light Kramers' degenerate valence bands) are accounted for. The wave functions were then forced to satisfy the two boundary conditions, necessitating the solution of an 8 × 8 determinant. Since we were anticipating that the band structure engineering would result in large (~ factor 2) changes in bandgap, it would have been incorrect to assume the usual fixed bulk values for the effective masses which depend reciprocally on the band gap. Instead an iterative procedure was employed in which the effective masses and the calculated bandgap were made mutually self-consistent. In our case this was particularly simple since we were targeting the band gap of $In_{0.53}Ga_{0.47}As$. We simply employed the effective masses of $In_{0.53}Ga_{0.47}As$. Under this philosophy, the Luttinger parameters were taken as equal in the well and in the barrier regions greatly simplifying the boundary conditions. In view of the need to make the calculation of the masses and bandgap self-consistent we believe that this procedure is justified.

The effect of the strain was accounted for by having a different well depth for the heavy hole, $m = \pm 3/2$ state from the light hole, $m = \pm 1/2$ state. The splitting between the two well depths is given simply by (6). The reason for such a simple way to account for the strain is that its uniaxial symmetry maintains the character of the $m = \pm 3/2$ heavy and the $m = \pm 1/2$ light hole wave functions. In the same way, if the barrier semiconductor on either side of the quantum well is strained, then the barrier level will be different for the two types of states.

Results of Calculations

The aim of these calculations was to map out the two dimensional band structure in strained InAs lattice matched to InP. Fig. 5 shows the results for a 50-Å-thick layer of the In-rich alloy $In_{0.77}Ga_{0.23}As$. We employed band structure and material parameters that were midway between those of $In_{0.53}Ga_{0.47}As$ and pure InAs as tabulated in Table I. The thickness and alloy composition were selected to target a bandgap appropriate to the 1.55 μm wavelength window of the SiO_2 glass fibers used in optical communications, i.e., a bandgap around 0.8 eV near that of $In_{0.53}Ga_{0.47}As$. The dashed line at the top of the valence band in Fig. 5 is what the heavy hole dispersion would look like in the absence of band structure engineering. The solid line HH1 is the calculated dispersion at the top of the engineered valence band. Notice that it forms a relatively sharp peak at the center of the dispersion curve. This is due to the repulsion of the LH1 band, and this sharp peaking has the important effect of producing a relatively small mass for holes at the top of the valence band. In fact this particular "nipple" shaped peak in the valence band is one of our major goals. Not only does the mass become relatively light at zone center, but there is a significant depression of the HH1 energy away from zone center. The difference in energy between the HH1 band and the dashed line away from zone center is 0.075 eV, or about 3 kT at room temperature. This brings about an e^{-3} reduction of heavy hole population due to the band structure engineering. As was discussed earlier in this article, the heavy holes are deleterious in three different ways. By reducing their thermal occupation by e^{-3} the intervalence band absorption shown in Fig. 2 should be reduced by the same factor. Similarly, the Auger recombination shown in Fig. 3 should be reduced by e^{-6} since two heavy holes must participate in the CHSH process. The sharp curvature at the top of the HH1 band results in an effective mass of $0.089m_e$ where m_e is the free electron mass. This is favourable for reducing the effective mass asymmetry as illustrated in Fig. 1. Therefore band structure engineering can indeed solve three of the major difficulties in semiconductor lasers. The main problem in the valence band structure of Fig. 5 is the small splitting between HH1 and HH2. The thermal occupation

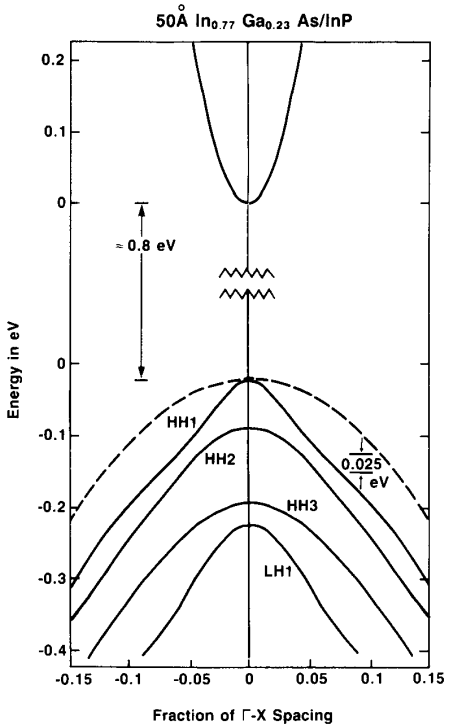

Fig. 5. The band structure calculated for a single 50-Å strained quantum well of $In_{0.77}Ga_{0.23}As$. The dispersion is in the plane of the well. The dashed line shows the normal heavy hole dispersion of $In_{0.53}Ga_{0.47}As$ which has a similar bandgap to the strained quantum well. The main point is the bump at zone center in the topmost valence band representing hole dispersion of mass $0.089m_e$ where m_e is the free electron mass. The off zone center heavy hole population is diminished by approximately e^{-3} due to the valence band shape.

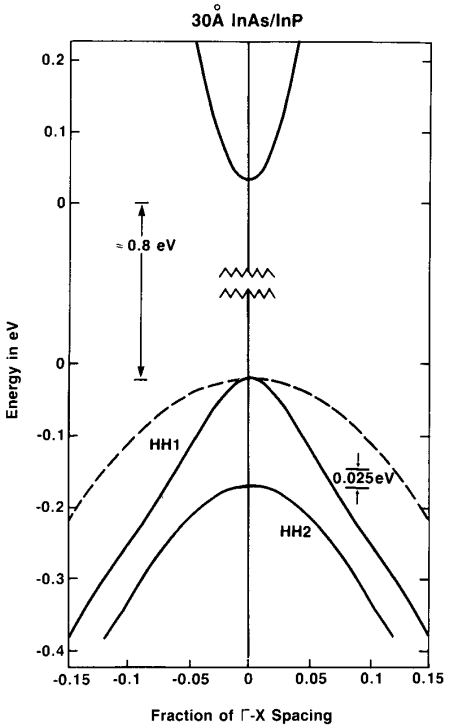

Fig. 6. This band structure approaches most closely the ideal band structure we would like to achieve. The hole mass is only $0.096m_e$, and the off zone center population is down by approximately e^{-5}. The only other subband in the problem HH2, is 0.2 eV away from the valence band edge and has negligible population at ambient temperatures. The dashed line is the bulk heavy hole dispersion.

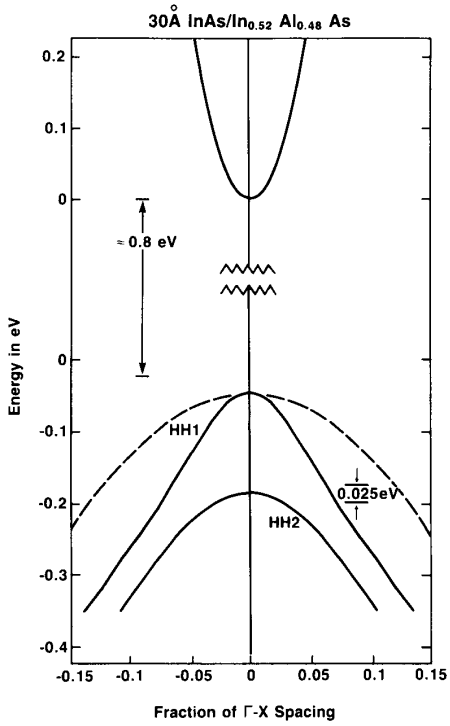

Fig. 7. $In_{0.52}Al_{0.48}As$ barrier layers produce the same favorable band structure as InP barrier layers. The hole mass is only $0.099m_e$. The dashed line is the bulk heavy hole dispersion.

of HH2 can result in the loss of some of our hard won benefits.

Therefore it makes sense for us to consider even thinner quantum wells as shown in Fig. 6. The increase in In composition to 100 percent reduces the bandgap which is balanced by the increase in bandgap due to the quantum size effect, primarily in the conduction band. The net effect is that the bandgap remains about the same, but the desirable effects on the valence band structure become even more pronounced. The "nipple" at the top of the HH1 band projects higher than before. The difference in energy between the dashed line and HH1 becomes ~ 0.125 eV resulting in an e^{-5} reduction in off zone center heavy hole population at room temperature. This reduces intervalence band absorption by e^{-5} and CHSH Auger recombination by e^{-10}. The splitting between HH1 and HH2 is 0.2 eV minimizing any thermal occupation of HH2. The effective mass in HH1 at zone center is $0.096m_e$ in this case. The LH1 band is not shown on Fig. 6 since its binding energy was so weak that it was only a few millivolts away from the bulk continuum of the InP barrier layer. This is only an approximation since we have neglected the effects of the spin orbit split off band which effectively repels LH1, diminishing the HH1-LH1 splitting [13], [14] from what is shown here. Within that limitation, it is interesting then to find that there are only two significant subbands in the valence band structure of these materials. The thin quantum well has simplified the band structure to that degree.

If $In_{0.52}Al_{0.48}As$ is used as the barrier layer, then the results are pretty much the same as the previous band structure, as shown in Fig. 7. The main difference in the input parameters is the valence band offset which is smaller for $In_{0.52}Al_{0.48}As$ than for InP. This does not have much effect, reducing the HH1-HH2 splitting slightly and raising the effective mass slightly to $0.099m_e$. Recent experiments on such strain-layers [14] are consistent with this band structure.

In the course of a parametric study of the importance of the VBO, we found that its main effect was to put an upper limit on the HH1-HH2 splitting, since the splitting could never exceed the well depth. Since a splitting of ~ 0.2 eV is desirable to minimize the thermal population of HH2 at room temperature, it suggests that a VBO of 0.2 eV is a minimal requirement. Any further increase in VBO seems to have very little effect, which suggests that our uncertainty in the numerical value of VBO is unimportant provided that it exceeds the minimal value. This is gratifying since the accuracy of the VBO numbers is not that good and the reliability of our calculations does not appear to depend so strongly on them.

Unfortunately, the InAs/GaAs VBO does not exceed the minimal requirements. In fact the valence band splitting of GaAs, which is not displayed on Fig. 4, means

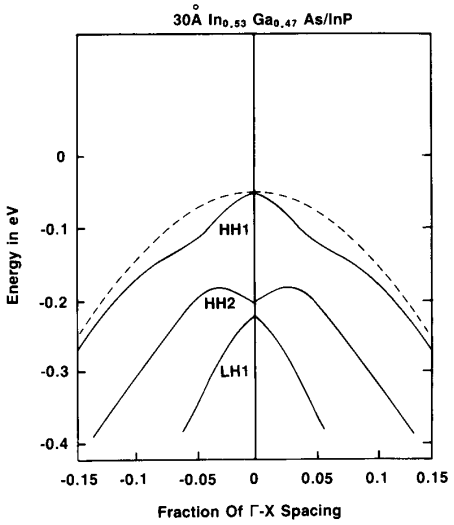

Fig. 8. The valence band structure of $In_{0.53}Ga_{0.47}As$ showing the effects of quantum confinement in the absence of strain. There is some change in shape of the topmost valence subband, but the overall energy shift compared to bulk heavy hole dispersion (dashed line), is relatively mild. The off zone center heavy hole population is only slightly reduced.

that there is no barrier [9] at all for the $m = \pm 1/2$ light band. Accordingly, we will not present any calculations employing $In_xGa_{1-x}As$ alloys as wide bandgap barrier layers. O'Reilly *et al.* [15] presented calculations similar to ours in which unstrained $In_{0.29}Ga_{0.71}As$ was used as the wide bandgap barrier layer. According to our considerations, the use of $In_xGa_{1-x}As$ alloys as wide bandgap barrier layers will act to limit the HH1–HH2 splitting due to the small VBO and permit significant thermal population of the barriers.

The importance of strain is illustrated in Fig. 8 where the quantum well has no strain at all. The effective mass at zone center is relatively small at $0.118m_e$, but the curvature of HH1 is such as to produce very little reduction in the off zone center heavy hole population. This can be seen from the narrow spacing between the dashed line and HH1 in Fig. 8. We must conclude that strain is necessary to fully optimize the band structure of quantum wells. There have been recent calculations [13], [14] of band edge positions in the strained alloy series $In_xGa_{1-x}As$ which are in reasonable agreement with the band edge positions calculated here. This is in spite of our neglect of repulsion from the spin orbit split off band.

Conclusions

Based on the above discussion, the shape of the valence band represented in Figs. 5–7 is favourable for reducing intervalence band absorption and Auger recombination. Whether this will actually manifest itself in terms of lower laser threshold current density depends on many factors. The Auger recombination is thought to represent about half the threshold current in well designed semiconductor lasers. The overall recombination is due to: a) Shockley–Read–Hall nonradiative lifetime τ, b) spontaneous radiative recombination B, and c) Auger recombination C:

$$\frac{dn}{dt} = -\left(\frac{n}{\tau} + Bn^2 + Cn^3\right). \tag{7}$$

We have addressed radiative [6] and Auger recombination, but the effort is wasted unless material quality as represented by the Shockley–Read–Hall nonradiative lifetime τ is adequate. Some recent measurements [16] show that good quality material is available, but this is not necessarily guaranteed without testing. The experimental results of Fischer *et al.* [17] on threshold currents of strained layer lasers were reasonably good, $J_{th} \sim 152$ A/cm^2, but might have been limited by material quality. It might be worthwhile to note that their aging tests contradict the oft-quoted presumption that strain layers must always suffer from rapid degradation in a laser application. In this connection, we believe that one successful result acts as an existence proof and outweighs numerous failures.

It is interesting to ask what is the optimum number of active layers in a strained quantum well laser. Typically the gain of bulk semiconductor material is ~ 200/cm when pumped to a reasonable level. The reduction in gain due to the low fill factor of a single quantum well in a much thicker optical mode would reduce the effective gain, but this would be compensated by the increased density of states in two dimensions. In practice these questions revolve around mirror reflectivity and other systems considerations. Nevertheless, there is no doubt that for the lowest threshold current only a single well should be employed and the mirror reflectivities should be adjusted to make that possible.

With regard to the lowest possible current threshold, it should be possible to make Auger and other nonradiative recombination negligible, leaving only spontaneous radiative recombination. As shown in [1] there is an almost unavoidable link between gain and spontaneous emission which is the link expressed by Einstein's A and B coefficients. In semiconductor lasers this expresses itself as:

$$J_{sp} = 8\pi q g d \Delta\nu / \lambda^2 \tag{8}$$

where q is the charge on the electron, g is the gross gain uncorrected for absorption, d is the effective thickness of the quantum well, $\Delta\nu$ is the spontaneous emission bandwidth, and λ the wavelength in the medium. For reasonable values of parameters in (8), it is possible to anticipate threshold current densities below 10 A/cm^2 suggesting further improvement over the values given in [17].

Acknowledgment

The authors would like to acknowledge valuable discussions with M.-H. Meynadier and to thank E. P. O'Reilly for making his manuscript [15] available before publication. They would also like to thank Jisoon Ihm for some preliminary calculations.

REFERENCES

[1] E. Yablonovitch and E. O. Kane, "Reduction of lasing threshold current density by the lowering of valence band effective mass," *J. Lightwave Technol.*, vol. LT-4, p. 504, 1986, also "Erratum," *J. Lightwave Technol.*, vol. LT-4, p. 961, 1986.

[2] A. R. Adams, "Band structure engineering for low threshold high efficiency semiconductor lasers," *Electron Lett.*, vol. 22, p. 249, 1986.

[3] G. C. Osbourn, R. M. Biefeld, and P. L. Gourley, "A GaAsP/GaP strained layer superlattice," *Appl. Phys. Lett.*, vol. 41, p. 172, 1982.

[4] M. G. A. Bernard and G. Duraffourg, "Laser conditions in semiconductors," *Phys. Stat. Solidi*, vol. 1, p. 699, 1961.

[5] S. M. Sze, *Physics of Semiconductor Devices*. New York: Wiley, 1961, p. 720.

[6] E. Yablonovitch, "Inhibited spontaneous emission in solid state physics and electronics," *Phys. Rev. Lett.*, vol. 58, p. 2059, 1987.

[7] O. Madelung, Ed., *Numerical Data and Functional Relationships in Science and Technology*, Group III, vol. 17. Berlin: Springer-Verlag, 1982.

[8] H. Kroemer, "Barrier control and measurements: Abrupt semiconductor heterojunctions," *J. Vac. Sci. Technol.*, vol. B2, p. 433, 1984.

[9] P. Voisin, M. Voos, J. Y. Marzin, M. C. Tamargo, R. E. Nahory and A. Y. Cho, "Luminescence investigations of highly strained-layer InAs-GaAs superlattices," *Appl. Phys. Lett.*, vol. 48, p. 1476, 1986.

[10] D. V. Lang, M. B. Panish, F. Capasso, J. Allam, R. A. Hamm, A. M. Sergent, and W. T. Tsang, "Measurement of heterojunction band offsets by admittance spectroscopy: $InP/In_{0.53}Ga_{0.47}As$," *Appl. Phys. Lett.*, vol. 50, p. 736, 1987.

[11] R. People, K. W. Wecht, K. Alavi, and A. Y. Cho, "Measurement of the conduction band discontinuity of molecular beam epitaxial grown $In_{0.53}Ga_{0.47}As/In_{0.52}Al_{0.48}As$ N-n heterojunction by C-V profiling," *Appl. Phys. Lett.*, vol. 43, p. 118, 1983.

[12] S. S. Nedorezov, "Space quantization in semiconductor films," *Sov. Phys. Solid State*, vol. 12, p. 1814, 1971.

[13] R. People, "Effects of coherency strain on the bandgap of psuedomorphic $In_yGa_{1-x}As$ on $\langle 100 \rangle InP$," *Appl. Phys. Lett.*, vol. 50, p. 1604, 1987.

[14] M. H. Meynadier, J.-L. de Miguel, M. C. Tamargo, and R. E. Nahory, "Optical investigations of the band structure of strained InAs/AlInAs quantum wells," *Appl. Phys. Lett.*, vol. 52, p. 302, 1988.

[15] E. P. O'Reilly, K. C. Heasman, A. R. Adams, and G. P. Witchlow, "Calculations of the threshold current and temperature sensitivity of a (GaIn)As strained quantum well laser operating at 1.55 μm," *Superlatt. Microstruct.*, vol. 3, p. 99, 1987.

[16] E. Yablonovitch, R. Bhat, J. P. Harbison, and R. A. Logan, "Survey of defect mediated recombination lifetimes in GaAs epilayers grown by different methods," *Appl. Phys. Lett.*, vol. 50, p. 1197, 1987.

[17] S. E. Fischer, D. Fekete, G. B. Feak, and J. M. Ballantyne, "Ridge waveguide injection laser with a GaInAs strained-layer quantum well ($\lambda = 1$ μm)," *Appl. Phys. Lett.*, vol. 50, p. 714, 1987.

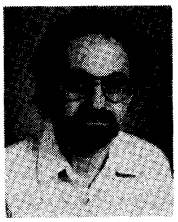

E. Yablonovitch graduated with the Ph.D. degree in applied physics from Harvard University in 1972.

He is presently a Member of the Technical Staff at Bell Communications Research, Red Bank, NJ. He has worked in the fields of nonlinear optics, laser-plasma interaction, infrared laser chemistry, and photovoltaic energy conversion. Currently his main interest is chemical modification of the electronic properties of semiconductors surfaces and photonic band structure.

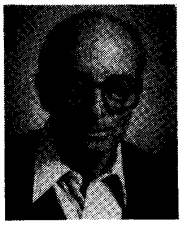

E. O. Kane received the Ph.D. degree in physics from Cornell University, Ithaca, NY, in 1953.

He was a Member of the Technical Staff at Bell Communications Research, Red Bank, NJ, specializing in semiconductor theory. He retired recently to spend more time with his grandchildren.